Cardiovascular Research (2015) **108**, 188–196
doi:10.1093/cvr/cvv202

Transmural APD gradient synchronizes repolarization in the human left ventricular wall

Bastiaan J. Boukens[1†], Matthew S. Sulkin[2†], Chris R. Gloschat[1], Fu Siong Ng[3], Edward J. Vigmond[4], and Igor R. Efimov[1,2,4*]

[1]Department of Biomedical Engineering, George Washington University, 5000 Science and Engineering Hall, 800 22ng Street NW, Washington, DC 20052, USA; [2]Department of Biomedical Engineering, Washington University, St. Louis, MO, USA; [3]National Heart and Lung Institute, Imperial College London, London, UK; and [4]Institut LIRYC, and Institut de Mathématiques de Bordeaux, Université de Bordeaux, Bordeaux, France

Received 7 November 2014; revised 13 July 2015; accepted 14 July 2015; online publish-ahead-of-print 24 July 2015

Time for primary review: 33 days

Aims The duration and morphology of the T wave predict risk for ventricular fibrillation. A transmural gradient in action potential duration (APD) in the ventricular wall has been suggested to underlie the T wave in humans. We hypothesize that the transmural gradient in APD compensates for the normal endocardium-to-epicardium activation sequence and synchronizes repolarization in the human ventricular wall.

Methods and results We made left ventricular wedge preparations from 10 human donor hearts and measured transmural activation and repolarization patterns by optical mapping, while simultaneously recording a pseudo-ECG. We also studied the relation between local timings of repolarization with the T wave *in silico*. During endocardial pacing (1 Hz), APD was longer at the subendocardium than at the subepicardium (360 ± 17 vs. 317 ± 20 ms, $P < 0.05$). The transmural activation time was 32 ± 4 ms and resulted in final repolarization of the subepicardium at 349 ± 18 ms. The overall transmural dispersion in repolarization time was smaller than that of APD. During epicardial pacing, the dispersion in repolarization time increased, whereas that of APD remained similar. The morphology of the T wave did not differ between endocardial and epicardial stimulation. Simulations explained the constant T wave morphology without transmural APD gradients.

Conclusion The intrinsic transmural difference in APD compensates for the normal cardiac activation sequence, resulting in more homogeneous repolarization of the left ventricular wall. Our data suggest that the transmural repolarization differences do not fully explain the genesis of the T wave.

Keywords Repolarization • T wave • Human • Optical mapping

1. Introduction

Prolongation and alterations in morphology of the T wave are associated with sudden cardiac death.[1] Despite a century having passed since the description of the T wave, the exact basis of this electrocardiographic waveform remains debated. Understanding the repolarization patterns that give rise to the T wave will contribute to early detection and diagnosis of cardiac electrical disorders.

The T wave is the result of asynchronous repolarization across the heart.[2] A large intrinsic gradient in action potential duration (APD) exists within the right and left ventricular walls, as observed in isolated left and right ventricular tissue preparations from humans and dogs.[3,4] It is thought that this gradient gives rise to the T wave recorded from these preparations and might even explain the T wave in the body surface ECG.[4,5] However, differences exist between a tissue preparation and the intact heart.[6] In intact dog and rabbit hearts, the transmural activation pattern compensates for the transmural difference in APD.[7,8] Therefore, the T wave observed in the ECG recorded from the intact mammal heart is thought to result from asynchronous ventricular repolarization along all the major anatomical axes.[9,10] In addition, the coupling of myocytes reduces intrinsic differences in repolarization properties.[11,12] The effect of the activation sequence and electrical coupling on synchronization of repolarization across the human ventricles is not well investigated.

In this study, we tested the hypothesis that the intrinsic transmural gradient in APD compensates for the normal endocardium-to-epicardium activation delay and synchronizes repolarization across the human left ventricular wall. We used human non-failing donor hearts that were rejected for transplantation from which we dissected left ventricular wedge preparations. We measured transmural

* Corresponding author. Tel: +1 202 9941635; fax: +1 202 9941635, Email: efimov@gwu.edu

† These authors contributed equally.

Published on behalf of the European Society of Cardiology. All rights reserved. © The Author 2015. For permissions please email: journals.permissions@oup.com.

activation and repolarization patterns by optical mapping and simultaneously recorded a pseudo-ECG. In addition, we used a computer model to test our hypothesis *in silico*. Our data indicate that the transmural gradient in APD compensates for the endocardium-to-epicardium activation sequence, leaving only a minor contribution, if any, of transmural repolarization to the genesis of the T wave.

2. Methods

In this study, we used 10 healthy non-failing donor hearts, provided by Mid-America Transplant Services (St. Louis, MO, USA), as described previously.[3] The procedures in this study were in accordance with legal regulations on the use of donor hearts in the USA. The Washington University School of Medicine Ethics Committee [Institutional Review Board (IRB)] approved the use of hearts that could not be used for transplantation purposes or for research purposes. Furthermore, the study performed conforms the declaration of Helsinki[13] and was approved by the Washington University IRB.

2.1 Experimental preparation

The hearts were cardioplegically arrested and cooled to +4–7°C in the operating room, immediately following cross-clamping of the aorta. The arrested hearts were maintained at +4–7°C to preserve the myocardium during the 15–20 min transportation from the operating room to the research laboratory.

We dissected left ventricular wedge preparations as described previously.[14] In brief, we isolated tissue preparations from the anterolateral left ventricular free wall supplied by a marginal branch of the circumflex artery, which was cannulated. Following the dissection, the preparations were placed into the optical mapping setup and perfused at 37°C with Tyrode's solution (in mmol/L): 128.2 NaCl, 4.7 KCl, 1.19 Na H_2PO_4, 1.05 $MgCl_2$, 1.3 $CaCl_2$, 27.0 $NaHCO_3$, and 11.1 glucose. pH was maintained at 7.4 by equilibration with a mixture of 95% O_2 and 5% CO_2. For recording of optical action potentials, we stained the preparations by perfusing with 10 μM di-4-ANEPPS (Molecular Probes, Eugene, OR, USA) for 10 min. The excitation–contraction uncoupler blebbistatin (10 μM, Tocris Bioscience, Ellisville, MO, USA) was added to the perfusate to remove motion artefacts. Excitation light was delivered by a 520 ± 5 nm light emitting diode (Prizmatix, Southfield, MI, USA), and emitted fluorescence was filtered >610 nm and recorded by a CMOS sensor (100 × 100 elements, 1 kHz, MICAM Ultima, SciMedia Ltd, Costa Mesa, CA, USA). A pseudo-electrocardiogram was recorded between two electrodes placed at the endocardial and epicardial sides at a distance of 3 cm from the wedge preparation (PowerLab 26T; AD-Instruments, Colorado Springs, CO, USA). Activation and repolarization patterns were measured during either endocardial ($n = 10$) or epicardial ($n = 5$) stimulation at pacing cycle lengths varying from 800 to 4000 ms.

2.2 Computer simulation

We generated a model of a tissue slab of 2 × 5 × 1 cm with a discretization of 200 μm, representing the average size of the human wedge preparations. We used the ten Tusscher human ventricular ionic model[15] for simulating the action potentials, and for the modelling conduction and repolarization patterns, we used the CARP simulator.[15] Potentials, calculated by summing the field contributions from the transmembrane currents, were determined 1.5 cm from the centres of the endocardial and epicardial faces and then subtracted to compute the pseudo-ECG.

2.3 Analysis

Optical action potentials were analysed with open source RHYTHM[16] software, which is based on MATLAB2012a (MathWorks Inc., Natick, MA, USA). For APD analysis, we averaged action potentials from an area of 1–2 mm^2. The local moment of activation (AT) was defined as the maximum positive d*V*/d*t* of the optical action potential, and to determine the moment of repolarization (RT), we estimated the negative d*V*/d*t* using 80% of repolarization.[17] To quantify the spatial homogeneity in repolarization, we constructed grey level co-matrices (GLCMs) using a function in Matlab2012.[18] A GLCM is built by calculating how often pairs of pixels with specific values and in a specified spatial relationship occur in a data set. Once the GLCM is constructed, statistical measures such as homogeneity can be calculated. Here, APD and RT values were scaled between 1 and 25 to create GLCM consisting of 25 rows and columns. The matrix entry GLCM(i, j) was constructed by calculating how often pixels with value i (1–25) were adjacent to a pixel with value j (1–25). The diagonal of GLCM represents optical data with similar APD and RT values that are in close proximity. The GLCM was normalized so that the sum of all the elements was equal to 1. The inhomogeneity index was calculated using the following equation:

$$H = 1 - \sum_{i,j} \frac{\mathrm{GLCM}(i,j)}{1 + |i - j|}$$

An inhomogeneity index value of 0 means that all the pixels in an optical map have the same value.

The start of the stimulus artefact was chosen to mark the beginning of ventricular activation, and the start and end of the T wave were defined via the tangent method.[19] The stimulus trigger was recorded in separate channels by both the optical and the electrical acquisition system and was used to align the two signals.

2.4 Statistics

Group comparisons were made using (repeated) analysis of variance. Values are given as mean ± SEM. A *P*-value of less than 0.05 was considered statistically different.

3. Results

3.1 Repolarization sequence in the left ventricular wall

We made left ventricular wedge preparations from 10 donor hearts. The characteristics of the donors are shown in *Table 1*. The thickness of the wall of the left ventricle varied between 9 and 14 mm. Pacing was applied at the endocardium. We mapped from the cut edge of the preparation to record transmural activation and repolarization sequences. We chose a field of view with activation isochrones parallel to the endocardium and epicardium, thereby mimicking the normal

Table 1 Clinical information ($n = 10$)

Age	Gender	Cause of death
11	Male	Anoxia
11	Female	Anoxia
73	Female	Cerebrovascular/stroke
61	Male	Cerebrovascular/stroke
50	Male	Intracranial haemorrhage/stroke
27	Male	Motor vehicle accident
57	Male	Intracranial haemorrhage/stroke
59	Male	Head trauma
54	Male	Cerebrovascular/stroke
48	Female	Cerebrovascular/stroke

transmural activation sequence (*Figure 1A*).[20] *Figure 1B* shows a typical example of the activation pattern of a left ventricular preparation during endocardial stimulation. The APD was the longest at the endocardial side and the shortest at the epicardial side, leading to a gradient in APD across the wall (*Figure 1C*). We could observe a clear difference in the moment of activation among the subendo, mid, and subepicardium, whereas a difference in the moment of repolarization was less evident (*Figure 1D*). Accordingly, reconstruction of the repolarization map showed a nearly homogenous repolarization pattern across the wall, instead of a transmural gradient (*Figure 1E*). This was a consistent finding in all preparations. On average, APD during 1 Hz pacing in the subendocardium was 360 ± 17 ms and in the subepicardium was 317 ± 20 ms, ΔAPD = 42 ± 6 ms. In comparison, the RT differed less, lasting 364 ± 16 ms in the subendocardium and 349 ± 19 ms in the subepicardium (*Figure 1F*), ΔRT = 15 ± 5 ms.

It has been reported that the midmyocardium contains myocytes with an extremely long action potential, especially at low cycle lengths.[4,5] These myocytes are referred to as 'M cells'. In our tissue preparations, the action potentials in the midmyocardium were never longer than those of the subendocardium at any cycle length (*Figure 1G*). Thus, we cannot confirm the existence of M cells.

3.2 Normal transmural activation sequence reduces heterogeneity in repolarization

For concordance of the QRS complex with the T wave, a negative correlation between the moment of activation and APD is required.[21,22] *Figure 2A* shows a typical example of the activation time (AT)−APD correlation in a representative tissue preparation. A negative correlation existed between AT and APD. As areas with short APDs activate late, it is expected that ΔRT is smaller than ΔAPD over a similar distance. To test this, we compared the inhomogeneity index (see Methods) of the APD with that of the RT. The RT was more homogeneously distributed than the APD (9 ± 2 vs. 13 ± 2, $P < 0.047$, *Figure 2B*).

To determine whether it was indeed the activation sequence that synchronized the gradient in APD, we reversed the order of activation by stimulating at the epicardium ($n = 5$) (*Figure 2C*). The correlation between AT and APD became positive during epicardial simulation. However, similar to endocardial pacing, the APD in the subendocardium remained longer than that in the subepicardium (389 ± 16 vs. 343 ± 38 ms, $P = 0.049$). The ΔRT between the subendocardium and the subepicardium, however, nearly tripled when compared with endocardial stimulation (16 ± 4 vs. 41 ± 4 ms). The latter suggests that the change in the activation sequence summed intrinsic APD differences and led to an increase in the dispersion of repolarization (*Figure 2E*). This was supported by the absence of a similar inhomogeneity index in the distributions of APD and RT during epicardial stimulation (17.2 ± 3 vs. 16.7 ± 3, $P = 0.54$, *Figure 2B*).

3.3 Relation between local repolarization moments and the T wave

To understand the mechanism underlying the genesis of the T wave, we recorded a pseudo-ECG from the wedge preparations. The T wave was biphasic for the majority of the preparations (9/10), and the QT (QTc) duration was, on average, 454 ± 26 ms at a pacing frequency of 60 b.p.m. (*Figure 3*). *Figure 4A* shows an example of a pseudo-ECG with subendocardial, subepicardial, apical, and basal action potentials. In this example, the basal region repolarized later than the apical region, whereas the subendocardium and subepicardium repolarized simultaneously. However, on average, repolarization times from the apical and basal regions were not different (*Figure 3*). It is evident that the end of repolarization measured on the transmural surface was never synchronous with the end of the T wave, which ended 112 ± 18 ms later. The duration of the T wave was 238 ± 21 ms, more than 10 times longer than ΔRT within the transmural surface (18 ± 6 ms). During epicardial stimulation, the QT interval (490 ± 33 ms) and T duration (290 ± 21) were longer than those during endocardial stimulation (*Figure 3*).

The observation that the end of the T wave did not coincide with repolarization on the transmural surface indicates that the myocardium outside the field of view, inside the tissue preparation, repolarized later. To record the last moment of repolarization, we stimulated the preparation from the other side of where we recorded optical action potentials (bottom, *Figure 4E* and *F*) at the endocardial/apical region. *Figure 4F* shows the activation and repolarization patterns during endocardial/apical/bottom stimulation. The last moment of repolarization was at the basal endocardial region and occurred closely to the end of the T wave.

The morphology of the T wave did not change when we switched from endocardial to epicardial stimulation or during stimulation on the bottom of the endocardial/apical/bottom region.

3.4 Modelling of the tissue preparation

So far, our data indicate that the myocardium repolarized later, outside our field of view. Therefore, we conducted a computer modelling study to simulate the activation and repolarization patterns that occurred there. We chose intrinsic APDs of 417 ms at the subendocardium and 340 ms at the subepicardium (*Figure 5A*). After coupling, APD reduced and produced a transmural gradient of 357 to 304 ms during endocardial stimulation, comparable to that measured in the wedge preparations (*Figure 5C*). During epicardial stimulation, the APD in the subendocardial region was shorter than that during endocardial stimulation, whereas the APD in the subepicardial region became longer (*Figure 5B*). We did not observe this phenomenon in our tissue preparations.

Complete activation of the tissue model occurred within 58 ms and was faster than the average QRS duration (72 ± 6 ms) recorded from our tissue preparations. The repolarization started at the mid-epicardium and ended at the bottom and top of the tissue model, thereby giving rise to a positive concordant T wave (*Figure 5D*). The T wave started before the first regions in the tissue slab reached RT80. To investigate whether potential difference led to the start of the T wave, we generated potential distributions at several time points (*Figure 5F*). At 80 ms after the onset of activation, there was a 4 mV potential difference throughout the tissue slab, which did not result in potential change on the pseudo-ECG. Shortly thereafter, the T wave started, which was the result of a small (7 mV) potential difference between the subendocardium and subepicardium. At $t = 300$ ms, the potential starts to rise faster, which was the result of a potential difference of 30 mV between subendocardium and subepicardium. At $t =$ 350 ms, the moment where the T wave had its maximum amplitude, the potential difference between the subendo and subepicardium was 81 mV. The end of the T wave did coincide with the last RT80 in the tissue slab.

Stimulation at the epicardium resulted in an opposite activation pattern within our experimental field of view (*x*-plane) (*Figure 6A*). However, in the *z*-plane, the activation front had the same direction.

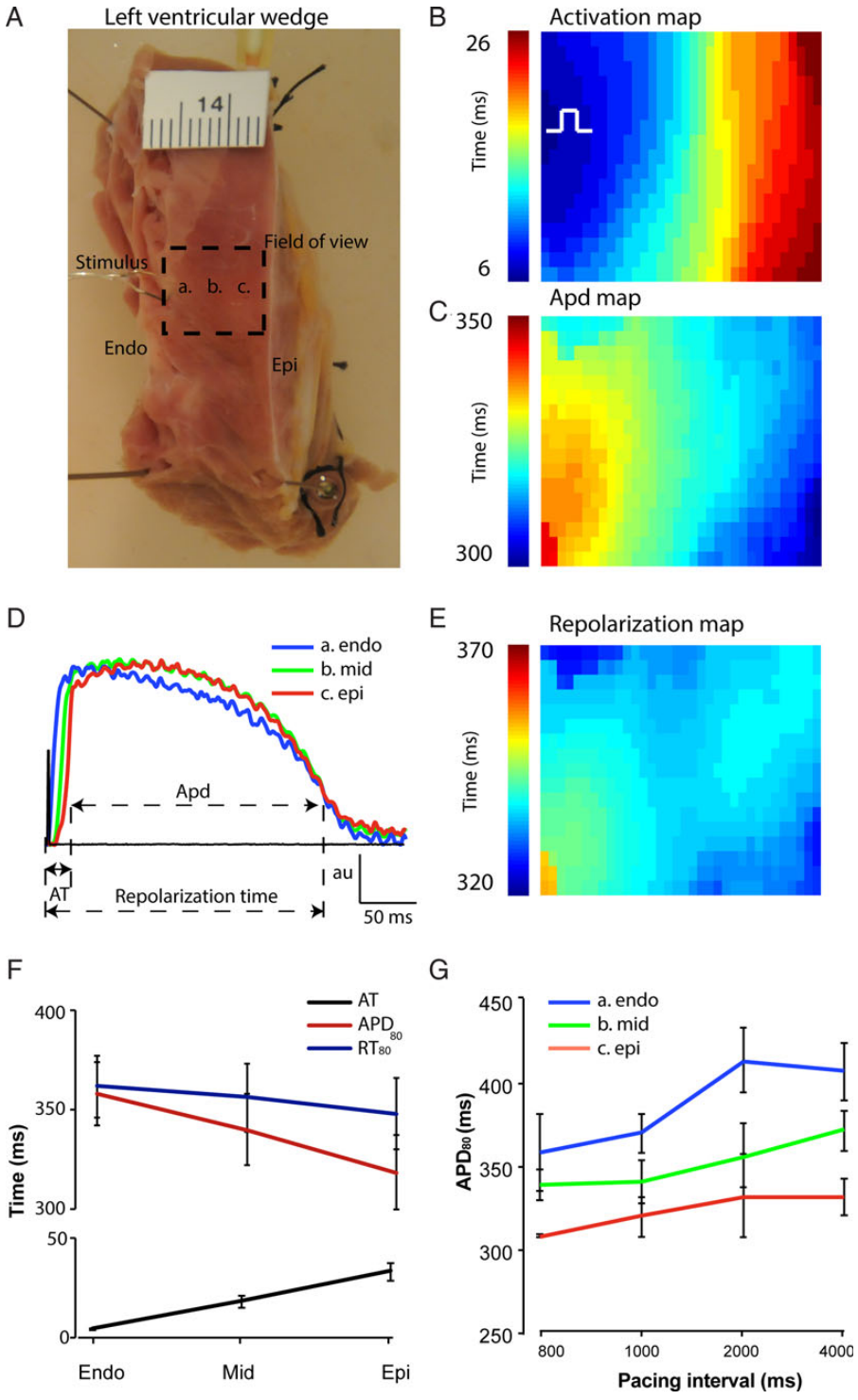

Figure 1 Gradient in APD and repolarization in the human left ventricular wall. (*A*) A photograph of a left ventricular tissue preparation. The dashed square represents the field of view and the letters a, b, and c correspond to the subendocardium, midmyocardium, and subepicardium, respectively. The ruler is in centimetres. (*B*) Activation pattern and (*C*) action potential gradient during endocardial stimulation within the field of view. The action potentials in (*D*) correspond to the area indicated by the letters in the photograph of (*A*). (*E*) Map shows the reconstructed repolarization gradient during endocardial stimulation. (*F*) The line graph shows the average APD and the local moment of activation and repolarization in the ventricular wall ($n = 10$). (*G*) The bar graph shows the average APD in the ventricular wall duration during different cycle lengths. Endo, subendocardial; Epi, subepicardial.

This most likely explains why the repolarization pattern during epicardial stimulation resembles the pattern during endocardial stimulation. This resulted in a T wave with a similar morphology during both epicardial and endocardial stimulations (*Figure 6B*). The duration of the T wave, however, was slightly longer during epicardial stimulation compared with endocardial stimulation.

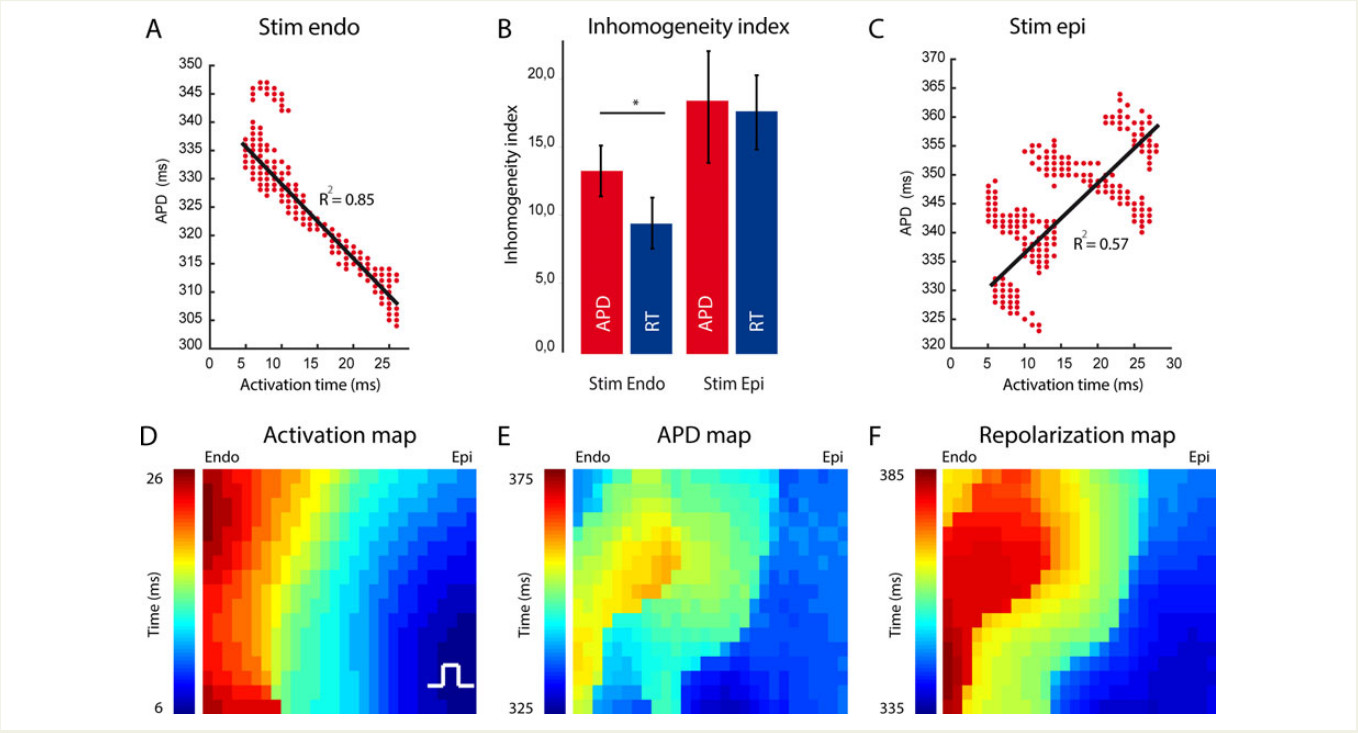

Figure 2 Relation between AT and APD during endocardial and epicardial stimulation. (*A* and *C*) The line graphs show the correlation between AT and APD and repolarization time during endocardial (*A*) and epicardial stimulation (*C*) ($n = 5$). (*B*) The bar graph shows the inhomogeneity level of APD and RT distribution during endocardial and epicardial stimulation. (*D*) Activation pattern within the field of view during epicardial stimulation. (*E*) Action potential gradient. (*F*) Repolarization pattern during epicardial stimulation. Endo, subendocardial; Epi, subepicardial.

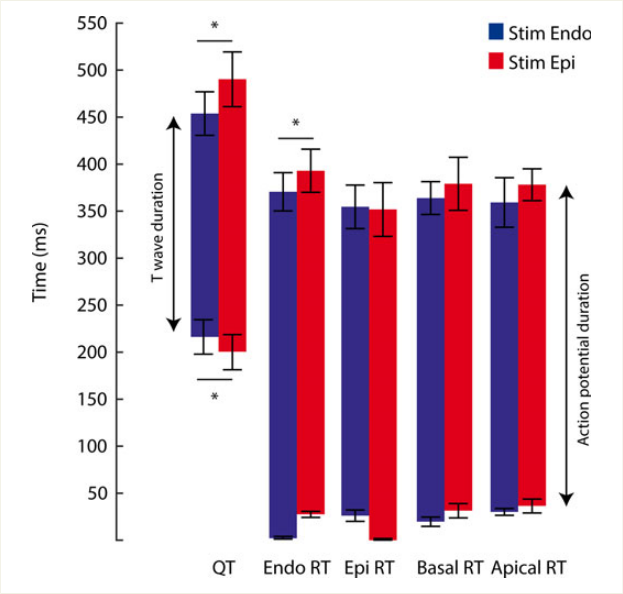

Figure 3 T wave in relation to local repolarization on transmural surface. The bar graph shows the QT interval calculated from pseudo-ECGs recorded from a left ventricular wedge preparation during endocardial and epicardial stimulation ($n = 5$). The repolarization times were calculated from simultaneously recorded optical action potentials. QT, QT interval; Endo, subendocardial; Epi, subepicardial; T, T wave.

3.5 The T wave in the wedge vs. the intact heart

The transmural activation pattern during point stimulation does not resemble that of normal activation in the intact heart, which is a line of activation from the endocardium to the epicardium throughout the ventricular wall.[20] Therefore, we simulated complete endocardial activation with line stimulation (*Figure 6C*). This resulted in a total AT of 23 ms. The difference in RT between the subendocardium and the subepicardium was 29 ms, which was longer than our experimental observations. The QT time and T wave duration were shorter than those during point stimulation from either the endocardium or the epicardium (*Figure 6B*). The T wave was longer than expected based on the difference in RT between the endocardium and the epicardium (90 vs. 32 ms). To compare the simulated T wave with that of the intact heart, we recorded an ECG from five healthy individuals at rest (see Methods). At a heart rate of 61 $\pm$ 4.4 b.p.m., the duration of the T wave was on average 178 $\pm$ 15 ms, which was more than twice as long as the T wave simulated during line stimulation (*Figure 6D*).

4. Discussion

Our data indicate that the transmural intrinsic differences in APD are largely attenuated by the normal endocardium-to-epicardium activation sequence, resulting in nearly homogeneous repolarization of the ventricular wall. Furthermore, the T wave recorded from a ventricular tissue preparation is not determined by transmural repolarization differences but rather by that of areas outside the field of view of the

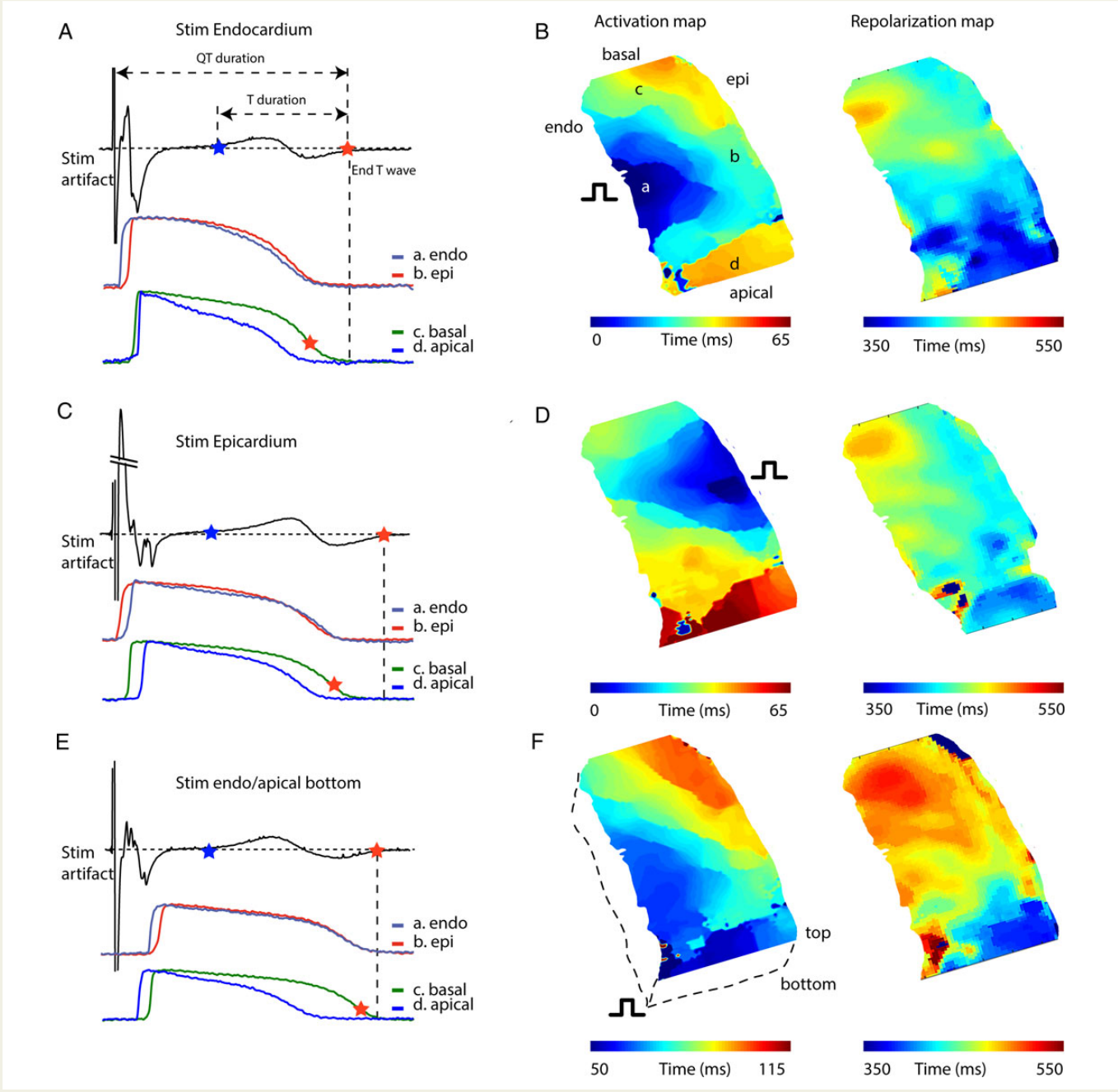

Figure 4 Relation between local repolarization and the T wave. (*A*, *C*, and *E*) A tracing of a pseudo-ECG (upper) recorded from a ventricular wedge preparation during endocardial stimulation along with simultaneously recorded optical action potentials (lower) from the subendocardium, subepicardium, basal, and apical myocardium during endocardial (*A*), epicardial (*C*), and endocardial/apical/bottom stimulation (*E*). (*B*, *D*, and *F*) Reconstructed activation (left) and repolarization (right) of the complete cut edge surface of a left ventricular wedge preparation during endocardial (*B*), epicardial (*D*), and endocardial/apical/bottom stimulation (*F*). Endo, subendocardial; Epi, subepicardial; T, T wave.

camera. Thus, our study provides novel insight into the role of transmural heterogeneity in repolarization in the genesis of the T wave.

4.1 Role of transmural heterogeneity in repolarization in the genesis of the T wave in the body surface ECG

We show in our tissue preparation that, during endocardial stimulation, the repolarization sequence proceeds opposite to the activation sequence. The difference in activation between the subendocardium and the subepicardium, however, is much larger than the difference in repolarization (32 ± 4 vs. 15 ± 5 ms, $P < 0.039$). During the normal transmural activation sequence, the transmural difference in repolarization results in a T wave duration of <90 ms. This indicates that the T wave recorded from the intact heart cannot solely be explained by a transmural difference in repolarization, which is supported by Meijborg *et al.*,[10] who recently showed that the T wave from the body surface ECG represents repolarization differences along multiple anatomic axes.

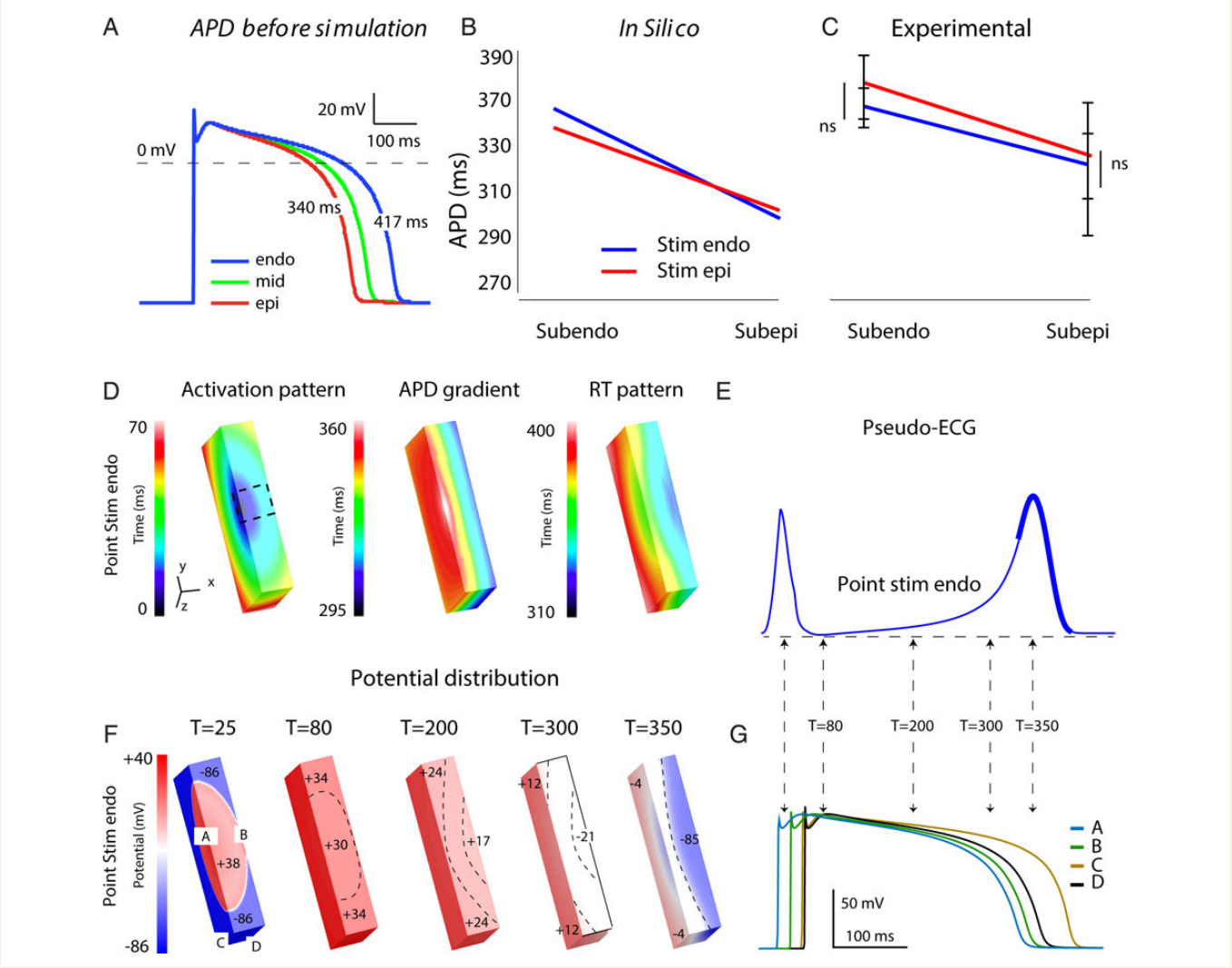

Figure 5 Simulation of the T wave recorded from left ventricular tissue preparation. (*A*) Action potentials at the endo, mid, and epicardium before simulation. The graphs show APD in the subendo and subepicardium of the tissue preparation during endocardial and epicardial stimulation *in silico* (*B*) and *ex vivo* (*C*). (*D*) The simulated activation sequence, action potential gradient, and repolarization pattern during endocardial point stimulation (*D*) in tissue slab representing the left ventricular tissue preparation. (*E*) The simulated pseudo-ECG during endocardial stimulation. (*F*) The potential distribution at $t = 25$ ms, $t = 80$ ms and $t = 200$ ms, $t = 300$ ms, and $t = 350$ ms during endocardial point stimulation. The numbers in the tissue slab indicate mV. (*G*) Action potentials at locations annotated in (*F*). Endo, subendocardial; Epi, subepicardial; *T*, time from onset activation.

Our experimental and simulation data show that the onset of the T wave preceded the first moments (phase 3 of the action potential) of repolarization and was caused by potential differences between the subendocardium and the subepicardium (*Figure 5F*). This is in concordance with one-dimensional modelling studies and three-dimensional experimental studies.[7,10,23] The importance of phases 1 and 2 of the action potential in the genesis of the T wave can also be deduced from the electric field formulation used to compute the ECG, which shows that all transmembrane potential gradients contribute to the genesis of the T wave.[24] This is important to consider when interpreting T waves with abnormal morphology.

4.2 Differences between our study and other wedge investigations

None of our 10 ventricular tissue preparations revealed the midmyocardial layer of myocytes known as M cells, which are characterized by prolonged APD relative to myocytes of the subendocardium and subepicardium. This contrasts with observations by Drouin *et al.*,[4,5] who showed that, in superfused transmural tissue slices of the human ventricle, the end of the T wave corresponds with the end of the action potential in the midmyocardium. We cannot explain the discrepancy between our results and the findings of Drouin *et al.* However, our data are in line with more recent studies of human ventricular myocardium, which also did not reveal a layer of M cells.[3,25–27] Glukhov *et al.*[3] and Lou *et al.*[28] did find, in a subset of their preparations (3 of 5 and 1 of 11, respectively), a small island of myocytes between the subendocardium and the midmyocardium with a longer APD than their neighbouring myocytes. We found in 1 out of 10 preparations that in a small region in the midmyocardial wall, the APD was ∼13 ms longer than that in the subendocardium. However, when a larger area was chosen to calculate the average APD, this difference disappeared. Walton *et al.*[29] showed that, in sheep, the Purkinje muscle junction can cause

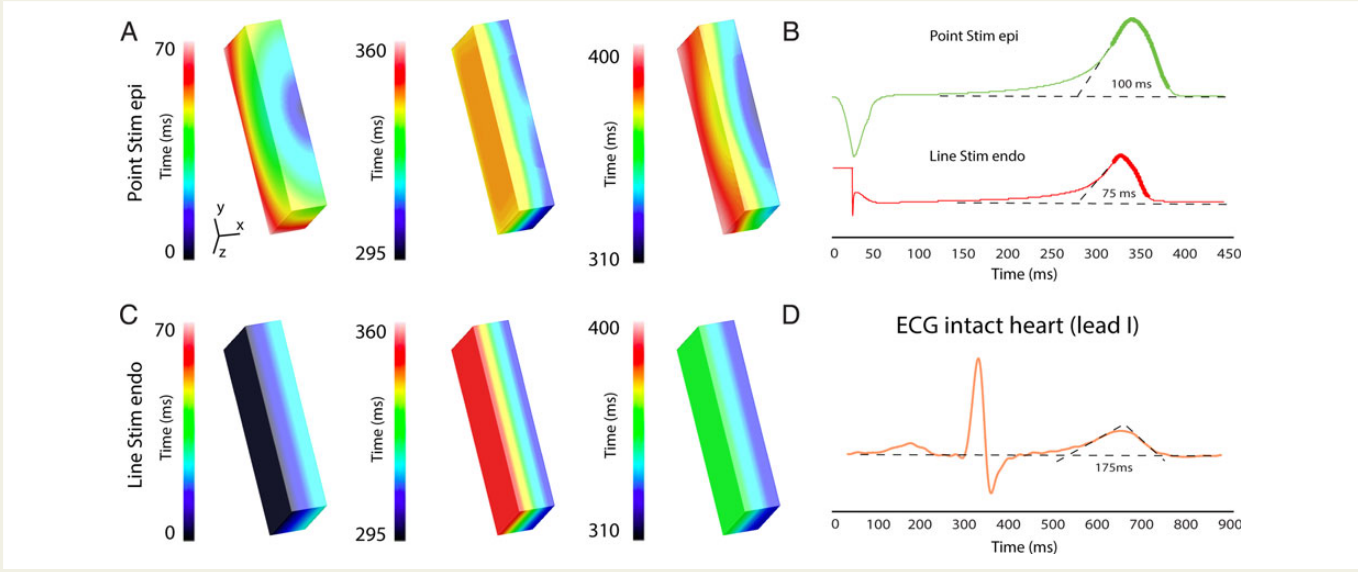

Figure 6 Simulation of transmural repolarization patterns during epicardial point and endocardial line stimulation. (*A*) The simulated activation sequence, action potential gradient, and repolarization pattern during epicardial point (*A*) and endocardial line (*C*) stimulation in tissue slab representing the left ventricular tissue preparation. (*B*) The simulated pseudo-ECG recorded from the different stimulation locations (*A*) and (*C*). (*D*) A representative example of a body surface ECG recorded from a healthy human. Endo, subendocardial; Epi, subepicardial.

local heterogeneity in APD. We posit that these Purkinje junctions may cause the long APD in the small islands observed by Glukhov *et al.*[3] The relevance of these regions for the genesis of the T wave in healthy human hearts, however, can be questioned as midmyocardium did not repolarize later than the subendocardium in neither their nor our study.

4.3 Transmural gradient in APD

It is thought that transmural repolarization gradients are absent or trivial in intact hearts.[6,7,9] The transmural sequence of activation is from endocardium to epicardium.[20] This must mean that there is a gradient in APD from endocardium to epicardium. This is exactly what we, and others, have found in the left ventricular wedge preparation. However, in intact hearts, gradients in APD (activation–recovery intervals) are not always found.[27]

Despite the positive AT–APD relation during epicardial stimulation, we found in two of five preparations small regions with a negative AT–APD relation during epicardial stimulation (*Figure 2C*). The reason for this observation is, in our opinion, that the endo-to-epi APD gradient is not linear throughout the cut surface. For example, in the top left of *Figure 2D*, the APD is shorter than that in the top mid. In this region, there is a negative correlation during epicardial stimulation. This region gives rise to the small group of data points observed in *Figure 2C*. However, in general, our data show that even when the subendocardium activates late and the epicardium activates early, the endo-to-epi APD gradient is still present. This indicates that the transmural gradient in APD is a characteristic of the myocardium. This is in contrast with studies in rabbit,[8] but in line with human studies on isolated myocytes and the reported transmural gradient in expression of ion channel genes that carry repolarizing currents.[30–32] The origin of this gradient is unknown and could have a developmental origin or be the result of cardiac memory or both.[33,34] The transmural gradient in APD should be taken into account when biventricular pacemaking is being considered for cardiac resynchronizing therapy because epicardial pacing increases the heterogeneity in repolarization. Such heterogeneity could be proarrhythmic.

For both the subendocardium and the subepicardium, there was no difference in APD between endocardial and epicardial stimulations. Based on electrotonic modulation, one would expect the APD to lengthen in the early activated regions and to shorten in the late activated regions.[12] A possible explanation could be that on the cutting surface of the tissue preparations, the area that we measure, the myocytes are slightly uncoupled and electrotonic modulation is reduced. This allows the subendocardium and the subepicardium to display their intrinsic APD and be less affected by the activation sequence.[35]

4.4 Biphasic T wave

We recorded a biphasic T wave from 9 of the 10 wedge preparations that we mapped. In these cases, the second part of the T wave had a negative polarity and was discordant with the RS complex (*Figure 4*). The observed morphology of the T wave likely resulted from the late activated areas and from the late repolarization that followed. The average QRS complex in the experiments was 72 ms and was longer than the QRS duration in the simulations (58 ms), indicating, indeed, that the total AT was longer than expected. We think that at the border zone of the perfused myocardium, for example, distal from the sutured arteries, the myocardium is slightly ischaemic and conduction slowed during the experiment. This is supported by the observation that the T wave often started as monophasic and concordant with the RS complex and then became biphasic after 10–15 min (data not shown).

4.5 Limitations

The use of a ventricular tissue preparation is a reductionist approach and a simplified representation of reality. Our tissue preparations came from the anterolateral area of the left ventricle, which may or may not represent the characteristics of the entire left ventricle, let alone those of the right ventricle. This should be taken into account

when applying our results to the functioning of an intact heart. Another point of critique is the use of Tyrode's solution, which might not provide full oxygenation compared with blood perfusion. Furthermore, the use of the excitation–contraction uncoupler blebbistatin may have altered repolarization. Finally, we measured optical action potentials at the cut surface where myocytes may be damaged and uncoupled, which could affect electrophysiological characteristics. However, APD in our tissue preparations corresponds to monophasic APD recorded from intact hearts, indicating the relevance of our model.[21]

5. Conclusion

In this study, we show that the transmural gradient in APD is attenuated by the activation sequence, resulting in almost homogenized repolarization of the ventricular wall. This means that the transmural difference in repolarization cannot explain the T wave morphology recorded from the intact heart. Furthermore, the T wave recorded from a ventricular tissue preparation is not the result of a transmural gradient in repolarization, but of early and late activated regions outside the field of view.

Acknowledgement

We thank Maria Efimova for critically reading the manuscript.

Conflict of interest: none declared.

Funding

The project was funded by NIH grant R01 HL114395 (I.R.E.). F.S.N. was supported by a British Heart Foundation Travel Fellowship (FS/11/69/29017) and a UK National Institute for Health Research Clinical Lectureship (LDN/007/255/A). E.J.V.: French government through ANR Investment of the Future grant ANR-10-IAHU-04.

References

1. Zhang L, Timothy KW, Vincent GM, Lehmann MH, Fox J, Giuli LC, Shen J, Splawski I, Priori SG, Compton SJ, Yanowitz F, Benhorin J, Moss AJ, Schwartz PJ, Robinson JL, Wang Q, Zareba W, Keating MT, Towbin JA, Napolitano C, Medina A. Spectrum of ST-T-wave patterns and repolarization parameters in congenital long-QT syndrome: ECG findings identify genotypes. *Circulation* 2000;**102**:2849–2855.
2. Franz MR, Bargheer K, Costard-Jackle A, Miller DC, Lichtlen PR. Human ventricular repolarization and T wave genesis. *Prog Cardiovasc Dis* 1991;**33**:369–384.
3. Glukhov AV, Fedorov VV, Lou Q, Ravikumar VK, Kalish PW, Schuessler RB, Moazami N, Efimov IR. Transmural dispersion of repolarization in failing and nonfailing human ventricle. *Circ Res* 2010;**106**:981–991.
4. Sicouri S, Antzelevitch C. A subpopulation of cells with unique electrophysiological properties in the deep subepicardium of the canine ventricle. *The M Cell Circ Res* 1991;**68**:1729–1741.
5. Drouin E, Charpentier F, Gauthier C, Laurent K, Le Marec H. Electrophysiologic characteristics of cells spanning the left ventricular wall of human heart: evidence for presence of M cells. *J Am Coll Cardiol* 1995;**26**:185–192.
6. Opthof T, Coronel R, Janse M, Rosen M. A wedge is not a heart. *Heart Rhythm* 2007;**8**:1116–1119.
7. Opthof T, Coronel R, Wilms-Schopman FJG, Plotnikov AN, Shlapakova IN, Danilo P, Rosen MR, Janse MJ. Dispersion of repolarization in canine ventricle and the electrocardiographic T wave: Tp-e interval does not reflect transmural dispersion. *Heart Rhythm* 2007;**4**:341–348.
8. Myles RC, Bernus O, Burton FL, Cobbe SM, Smith GL. Effect of activation sequence on transmural patterns of repolarization and action potential duration in rabbit ventricular myocardium. *Am J Physiol Heart Circ Physiol* 2010;**299**:H1812–H1822.
9. Janse MJ, Coronel R, Opthof T, Sosunov EA, Anyukhovsky EP, Rosen MR. Repolarization gradients in the intact heart: transmural or apico-basal? *Prog Biophys Mol Biol* 2012;**109**:6–15.
10. Meijborg VM, Conrath CE, Opthof T, Belterman CN, de Bakker JM, Coronel R. Electrocardiographic T wave and its relation with ventricular repolarization along major anatomical axes. *Circ Arrhythm Electrophysiol* 2014;**7**:524–531.
11. Defauw A, Kazbanov IV, Dierckx H, Dawyndt P, Panfilov AV. Action potential duration heterogeneity of cardiac tissue can be evaluated from cell properties using Gaussian Green's function approach. *PLoS ONE* 2013;**8**:e79607.
12. Walton RD, Benson AP, Hardy ME, White E, Bernus O. Electrophysiological and structural determinants of electrotonic modulation of repolarization by the activation sequence. *Front Physiol* 2013;**4**:281.
13. World Medical Association Declaration of Helsinki. Recommendations guiding physicians in biomedical research involving human subjects. *JAMA* 1997;**277**:925–926.
14. Di Diego JM, Sicouri S, Myles RC, Burton FL, Smith GL, Antzelevitch C. Optical and electrical recordings from isolated coronary-perfused ventricular wedge preparations. *J Mol Cell Cardiol* 2013;**54**:53–64.
15. ten Tusscher KH, Panfilov AV. Alternans and spiral breakup in a human ventricular tissue model. *Am J Physiol Heart Circ Physiol* 2006;**291**:H1088–H1100.
16. Laughner JI, Ng FS, Sulkin MS, Arthur RM, Efimov IR. Processing and analysis of cardiac optical mapping data obtained with potentiometric dyes. *Am J Physiol Heart Circ Physiol* 2012;**303**:H753–H765.
17. Potse M, Vinet A, Opthof T, Coronel R. Validation of a simple model for the morphology of the T wave in unipolar electrograms. *Am J Physiol Heart Circ Physiol* 2009;**297**:H792–H801.
18. Haralick RM, Shanmugam K, Itshak D. Textural features for image classification. *IEEE Trans Syst Man Cybern* 1973;**SMC-6**:11.
19. Lepeschkin E, Surawicz B. The measurement of the Q-T interval of the electrocardiogram. *Circulation* 1952;**6**:378–388.
20. Durrer D, Van Dam RT, Freud GE, Janse MJ, Meijler FL, Arzbaecher RC. Total excitation of the isolated human heart. *Circulation* 1970;**41**:899–912.
21. Franz MR, Bargheer K, Rafflenbeul W, Haverich A, Lichtlen PR. Monophasic action potential mapping in human subjects with normal electrocardiograms: direct evidence for the genesis of the T wave. *Circulation* 1987;**75**:379–386.
22. Cowan JC, Hilton CJ, Griffiths CJ, Tansuphaswadikul S, Bourke JP, Murray A, Campbell RW. Sequence of epicardial repolarisation and configuration of the T wave. *Br Heart J* 1988;**60**:424–433.
23. Gima K, Rudy Y. Ionic current basis of electrocardiographic waveforms: a model study. *Circ Res* 2002;**90**:889–896.
24. Plonsley RB, Roger C. *Bioelectricity: A Quantitative Approach*. New York, NY: Plenum Press; 1988, p149–163.
25. Ng FS, Holzem KM, Koppel AC, Janks D, Gordon F, Wit AL, Peters NS, Efimov IR. Adverse remodeling of the electrophysiological response to ischemia–reperfusion in human heart failure is associated with remodeling of metabolic gene expression. *Circ Arrhythm Electrophysiol* 2014;**7**:875–882.
26. Glukhov AV, Fedorov VV, Kalish PW, Ravikumar VK, Lou Q, Janks D, Schuessler RB, Moazami N, Efimov IR. Conduction remodeling in human end-stage nonischemic left ventricular cardiomyopathy. *Circulation* 2012;**125**:1835–1847.
27. Taggart P, Sutton PM, Opthof T, Coronel R, Trimlett R, Pugsley W, Kallis P. Transmural repolarisation in the left ventricle in humans during normoxia and ischaemia. *Cardiovasc Res* 2001;**50**:454–462.
28. Lou Q, Fedorov VV, Glukhov AV, Moazami N, Fast VG, Efimov IR. Transmural heterogeneity and remodeling of ventricular excitation–contraction coupling in human heart failure. *Circulation* 2011;**123**:1881–1890.
29. Walton RD, Martinez ME, Bishop MJ, Hocini M, Haissaguerre M, Plank G, Bernus O, Vigmond EJ. Influence of the Purkinje-muscle junction on transmural repolarization heterogeneity. *Cardiovasc Res* 2014;**103**:629–640.
30. Zicha S, Xiao L, Stafford S, Cha TJ, Han W, Varro A, Nattel S. Transmural expression of transient outward potassium current subunits in normal and failing canine and human hearts. *J Physiol* 2004;**561**:735–748.
31. Nabauer M, Beuckelmann DJ, Uberfuhr P, Steinbeck G. Regional differences in current density and rate-dependent properties of the transient outward current in subepicardial and subendocardial myocytes of human left ventricle. *Circulation* 1996;**93**:168–177.
32. Gaborit N, Le Bouter S, Szuts V, Varro A, Escande D, Nattel S, Demolombe S. Regional and tissue specific transcript signatures of ion channel genes in the non-diseased human heart. *J Physiol* 2007;**582**:675–693.
33. Rosenbaum MB, Blanco HH, Elizari MV, Lazzari JO, Davidenko JM. Electrotonic modulation of the T wave and cardiac memory. *Am J Cardiol* 1982;**50**:213–222.
34. Boukens BJ, Christoffels VM, Coronel R, Moorman AF. Developmental basis for electrophysiological heterogeneity in the ventricular and outflow tract myocardium as a substrate for life-threatening ventricular arrhythmias. *Circ Res* 2009;**104**:19–31.
35. Joyner RW, Picone J, Veenstra R, Rawling D. Propagation through electrically coupled cells. Effects of regional changes in membrane properties. *Circ Res* 1983;**53**:526–534.